Molecular Pharmacology Fast Forward. Published on January 19, 2018 as DOI: 10.1124/mol.117.111146
This article has not been copyedited and formatted. The final version may differ from this version.



# Activation of constitutive androstane receptor ameliorates renal ischemia-reperfusion induced kidney and liver injury

You-Jin Choi, Dong Zhou, Anne Caroline S. Barbosa, Yongdong Niu, Xiudong Guan, Meishu Xu, Songrong Ren, Thomas D. Nolin, Youhua Liu, Wen Xie

Center for Pharmacogenetics and Department of Pharmaceutical Sciences (Y.J.C., A.C.B., Y.N, M.X., S.R., W.X.), Department of Pathology, School of Medicine (D.Z., Y.L.), Center for Clinical Pharmaceutical Sciences, Department of Pharmacy and Therapeutics, School of Pharmacy (T.D.N) and Department of Pharmacology and Chemical Biology (W.X.) University of Pittsburgh, Pittsburgh, Pennsylvania, USA, Department of Pharmacology, Shantou University Medical College, Shantou, Guangdong, China (Y.N.) and Department of Neurosurgery, Beijing Tiantan Hospital, Capital Medical University, Beijing, China (X.G.).

**Running title:** CAR ameliorates AKI-induced liver injury

[#]**Corresponding author:** Center for Pharmacogenetics and Department of Pharmaceutical Sciences, 306 Salk Pavilion, University of Pittsburgh, Pittsburgh, PA 15261. E-mail: wex6@pitt.edu

Number of text pages: 32

Number of figures: 8

Number of references: 46

Number of words in Abstract: 246

Number of words in Introduction: 710

Number of words in Discussion: 1059

**Abbreviations**

AKI, acute kidney injury; BUN, blood urea nitrogen; CAR, constitutive androstane receptor; CKD, chronic kidney disease; IR, ischemia-reperfusion; MTTP, microsomal triglyceride transfer protein; NGAL, neutrophil gelatinase-associated lipocalin; TCPOBOP, 1,4-bis[2-(3,5 dichloropyridyloxy)] benzene; TUNEL, terminal transferase dUTP nick end labeling; VLDL-TG, very low-density lipoprotein-triglyceride

## Abstract

Acute kidney injury (AKI) is associate with high mortality. Despite the evidence of AKI-induced distant organ injury, a relationship between AKI and liver injury has not been clearly established. The goal of this study is to investigate whether renal ischemia-reperfusion (IR) can affect liver pathophysiology. We showed that renal IR in mice induced fatty liver and compromised liver function through the down-regulation of constitutive androstane receptor (CAR; -90.4%) and inhibition of hepatic very low-density lipoprotein-triglyceride (VLDL-TG) secretion (-28.4%). Treatment of mice with the CAR agonist 1,4-bis[2-(3,5 dichloropyridyloxy)] benzene (TCPOBOP) prevented the development of AKI-induced fatty liver and liver injury, which was associated with the attenuation of AKI-induced inhibition of VLDL-TG secretion. The hepato-protective effect of TCPOBOP was abolished in $CAR^{-/-}$ mice. Interestingly, alleviation of fatty liver by TCPOBOP also improved the kidney function, whereas CAR ablation sensitized mice to AKI-induced kidney injury and lethality. The serum concentrations of IL-6 were elevated by 27-fold after renal IR, but were normalized in TCPOBOP-treated AKI mice, suggesting that the increased release of IL-6 from the kidney may have mediated the AKI responsive liver injury. Taken together, our results have revealed an interesting kidney-liver organ crosstalk in response to AKI. Given the importance of CAR in the pathogenesis of renal IR-induced fatty liver and impaired kidney function, fatty liver can be considered as an important risk factor for kidney injury and a timely management of hepatic steatosis by CAR activation may help to restore kidney function in patients with AKI or kidney transplant.

## Introduction

Acute kidney injury (AKI) is one of the serious complications of critical illness that is associated with significant mortality (Rewa and Bagshaw, 2014). AKI is characterized by the sudden impairment of kidney function, as measured by serum creatinine and urine volume (Khwaja, 2012), resulting in the retention of waste products. Ischemia is a common cause of AKI, which can occur in many clinical situations, such as renal transplantation, partial nephrectomy, heart surgery, and hypoperfusion associated with sepsis. Hallmarks of ischemic AKI include inflammation, disruption of the apical brush border of tubular cells, and death of the renal tubular epithelial cells (Devarajan, 2006; Wu et al., 2007). Previous studies have shown that apoptosis and necrosis mainly occur in tubular epithelial cells following ischemic AKI (Shi et al., 2000). While ischemia-induced kidney injury has been well documented, the effects of renal ischemia on distant organs need further investigation.

Earlier studies have suggested organ cross-talk between the injured kidney and distant organs, such as the lungs, liver, heart, gut, and brain (Doi and Rabb, 2016). More recent data highlight the importance of immune response, activation of inflammatory cascades, and an alteration of transcriptional events in distant organs during the renal injury. Hepatic dysfunction has been reported in patients suffering from AKI (Chertow et al., 1995). Liver injury after the ischemic renal injury or nephrectomy is characterized by hepatocyte vacuolization, necrosis, and apoptosis with inflammatory changes (Park et al., 2011; Park et al., 2012). Several studies have suggested mechanisms for the interaction between the injured kidney and liver. In one example, renal injury increased the intestinal expression of IL-17A and caused small intestinal injury (Park et al., 2011). These events resulted in hepatic inflammation and increased the release of TNFα and IL-6 from the liver into the circulation. Reactive oxygen species and oxidative stress are also important players in AKI-induced liver

injury. Renal ischemia-reperfusion (IR) reduces glutathione levels in the liver and blood through the inhibition of glutamate-cysteine ligase, the first rate-limiting enzyme of glutathione synthesis (Shang et al., 2016). Lipid peroxidation is also increased in the liver as evidenced by the elevated level of malondialdehyde. In contrast, administration of glutathione protects the liver from renal IR-induced injury, which was associated with decreased levels of malondialdehyde (Golab et al., 2009).

AKI can resolve naturally, but if not, it may progress to chronic kidney disease (CKD; (Venkatachalam et al., 2015). The relationship between CKD and fatty liver has been controversial. Obesity, insulin resistance, diabetes, and hypertension are shared risk factors in the development of both CKD and fatty liver (Targher and Byrne, 2017). Several cross-sectional and longitudinal studies suggest that fatty liver is associated with an increased prevalence of CKD (Musso et al., 2014). Moreover, the severity of fatty liver is associated with an increased risk of CKD in diabetic and non-diabetic patients. Meanwhile, CKD may contribute to the development of fatty liver and insulin resistance (Axelsson et al., 2011; Pelletier et al., 2013).

The constitutive androstane receptor (CAR) was initially characterized as a xenobiotic nuclear receptor regulating a mammal's responses to xenotoxicants (Honkakoski et al., 1998; Wei et al., 2000). Recently results, including those published from our laboratory, have implicated this receptor in the control of energy metabolism, including the inhibition of lipogenesis (Gao and Xie, 2012). Activation of CAR inhibited hepatic steatosis in both the high-fat diet and ob/ob obese models (Gao et al., 2009). Activation of CAR has also been shown to relieve hepatic injuries, such as those caused by cholestasis and hyperbilirubinemia, through increased metabolism and excretion of endogenous and exogenous toxins. The

Molecular Pharmacology Fast Forward. Published on January 19, 2018 as DOI: 10.1124/mol.117.111146
This article has not been copyedited and formatted. The final version may differ from this version.



expression and activity of CAR can be suppressed by inflammation (Assenat et al., 2004; Pascussi et al., 2000). Knowing that acute inflammatory response is an integral component in the pathogenesis of AKI, it is interesting to know whether and how CAR plays a role in the kidney-liver crosstalk in the context of AKI.

In this study, we uncovered a novel function of CAR in mediating the kidney-liver crosstalk in AKI. Renal IR down-regulated the expression and activity of CAR and decreased the expression of microsomal triglyceride transfer protein (MTTP), which resulted in a decreased VLDL-TG secretion and lipid accumulation and liver injury. Pharmacological activation of CAR alleviated IR-induced fatty liver and liver injury, leading to improved renal function.

Molecular Pharmacology Fast Forward. Published on January 19, 2018 as DOI: 10.1124/mol.117.111146
This article has not been copyedited and formatted. The final version may differ from this version.



## Materials and Methods

### *Animals, animal surgery and drug treatments*

Eight-week-old male C57BL/6 mice were purchased from Jackson Laboratory (Bar Harbor, ME). The creation of $CAR^{-/-}$ mice has been described previously (Wei et al., 2000). Mice were maintained ad libitum in a temperature-controlled animal facility. To induce renal IR-induced AKI, both kidneys were clamped to block blood flow for 30 min. After ischemia, clamps were released to start reperfusion and mice were sacrificed after 24 h or 48h. For studying the effect of CAR activation, the mice were randomly assigned, and treatment groups were administered with TCPOBOP (1 mg/kg BW/day; i.p.) for two days before the renal IR surgery. Vehicle groups received the same volume of corn oil. All chemicals were ordered from Sigma Aldrich (St. Louis, MO). The use of animals complied with the guidelines established by the Institutional Animal Care and Use Committee (IACUC) of the University of Pittsburgh.

### *Histological analysis*

The kidney and liver tissues were fixed in 10% neutral buffered formalin for 24 h and then dehydrated, embedded in paraffin, sectioned at 4 μm, and stained with hematoxylin and eosin (H&E) for general histology. Immunostaining was performed on the paraffin sections. Slides were incubated overnight with the primary anti-CAR antibody (sc-13065) from Santa Cruz Biotechnology (Santa Cruz, CA) diluted to 1:100 at 4°C in humid chambers and were counterstained with hematoxylin. To detect lipid deposits in the liver, liver tissues were embedded in Tissue-Tek OCT compound (Sakura Finetek, Torrance, CA), and cryosections (8 μm) were prepared and stained with Oil-Red O. TUNEL staining was performed by using the In Situ Cell Death Detection Kit from Roche Molecular Biochemicals (Mannheim, Germany). In brief, paraffin sections were treated with the TUNEL enzyme solution and counterstained

with DAPI. The slides were immediately evaluated by fluorescence microscopy for positively stained necrotic nuclei.

***Serum and tissue biochemistry***

Serum was separated from blood by low-speed centrifugation (1,500 g, 10 min, 4°C), transferred into aliquots, and stored at −80°C until analysis. Serum creatinine and BUN levels were evaluated with the QuantiChrom™ Creatinine Assay Kit and the QuantiChrom™ Urea Assay Kit (BioAssay System, Hayward, CA), respectively. The serum levels of ALT, AST (Stanbio Laboratory, Boerne, TX) and total bilirubin (Sigma Aldrich) were measured by using commercial assay kits. The concentrations of IL-6 were measured by an ELISA kit from R&D Systems (Minneapolis, MN). To measure hepatic lipid contents, liver lipids were extracted from homogenate prepared from 100 mg of tissue using chloroform/methanol mix (2:1, v/v). Triglycerides and cholesterol levels in the liver lipid extracts and serum were determined using colorimetric assay kits from Stanbio Laboratory.

***Western blot analysis***

Liver and kidney tissue lysates were prepared by homogenization using lysis buffer (50 mM HEPES, 150 mM NaCl, 1% Triton X-100, 5 mM EGTA, 50 mM glycerophosphate, 20 mM NaF, 1 mM Na3VO4 and 2 mM PMSF) and centrifuged at 12,000 rpm for 10 min. Supernatants were collected, electrophoresed on 8-15% SDS-PAGE and transferred onto PVDF membrane (Millipore, Bedford, MA). Western blots were probed with the following antibodies: CAR (sc-13065), MTTP (sc-135994) and Apob100 (sc-12332) from Santa Cruz, NGAL (MAB1857) from R&D Systems, Caspase 3 (#9662) from Cell Signaling Technology (Beverly, MA), and β-actin (A1978) from Sigma Aldrich. Detection was performed by enhanced chemiluminescence using a Thermo ECL kit from Thermo Fisher (Waltham, MA).

Molecular Pharmacology Fast Forward. Published on January 19, 2018 as DOI: 10.1124/mol.117.111146
This article has not been copyedited and formatted. The final version may differ from this version.



***RNA isolation and quantitative real-time PCR (qRT-PCR)***

Total RNA was isolated using the TRIZOL reagent. RNase-free DNase I treated total RNA was used to synthesize single-strand cDNA. A quantitative real-time PCR was performed on an ABI 7300 Real-Time PCR System (Applied Biosystems, Foster City, CA). The primer sequences for the mouse *Car* are 5′-GGAGCGGCTGTGGAAATATTGCAT-3′ and 5′-TCCATCTTGTAGCAAAGAGG CCCA-3′. The primer sequences for the mouse *Cyp2b10* are 5′-GCATTTGTCTTGGTGAAAGCATT-3′ and 5′-GGATGGACGTGAAGAAAAGGAA-3′. The primer sequences for the mouse *Il-6* are 5′-CGACGGCCTTCCCTACTT-3′ and 5′-TGGGAGTGGTATCCTCTGTGAA-3′. Melting curve analysis was performed to determine the specificity of amplification. Relative changes in gene expression were expressed as the fold change using the $2^{-\Delta\Delta CT}$. Gene expression was normalized to the expression of the control cyclophilin gene.

***Very low-density lipoprotein-triglyceride (VLDL-TG) secretion assay***

After 4h fasting, mice were administered with an intravenous injection of tyloxapol from Sigma Aldrich at 500 mg/kg body weight. Blood samples were collected from the tail vein at 0, 30, 60, and 120 min after the tyloxapol injection and plasma triglyceride levels were measured.

***Transient transfection and luciferase reporter gene assay***

The pCMX-HA-mCAR and tk-PBRE constructs were described previously (Xie et al., 2000). HEK293T cells were transiently transfected with pCMX-HA-mCAR and tk-PBRE plasmids by using the Lipofectamine 2000 from Invitrogen. The pCMX-β-gal plasmid was added as an internal control to monitor the transfection efficiency. After transfection, cells were incubated

Molecular Pharmacology Fast Forward. Published on January 19, 2018 as DOI: 10.1124/mol.117.111146
This article has not been copyedited and formatted. The final version may differ from this version.



with IL-6 (50 U/ml) with DMSO or TCPOBOP (200 nM) for 24h. The luciferase activity was normalized with the β-gal activity.

***Statistical analysis***

All data were expressed as mean ± SD. Statistical analysis was performed using Student's *t*-test or two-way analysis of variance (ANOVA) where appropriate. Differences between groups were considered to be statistically significant at $p < 0.05$. Multiple comparisons were evaluated by two-way ANOVA followed by Tukey's multiple comparison tests.

Molecular Pharmacology Fast Forward. Published on January 19, 2018 as DOI: 10.1124/mol.117.111146
This article has not been copyedited and formatted. The final version may differ from this version.



## Results

### *Renal IR induces hepatic steatosis*

We established an ischemia-reperfusion based mouse model of AKI in order to determine whether AKI alters the pathophysiology of the liver. In this model, both kidneys were clamped for 30 min and then reperfused for 24 h. The kidney function was evaluated by serum creatinine and BUN levels. Renal IR led to significant rises in serum creatinine and BUN levels as expected (Fig. 1A). Compared to the normal renal structure in the sham group, the AKI group showed signs of severe renal pathological changes, such as loss of tubular cell brush border, tubular dilatation, and necrosis (Fig. 1B). Next, we examined the liver, liver histology, and liver function. Unexpectedly, the livers of AKI mice were pale in color, and appeared fatty (Fig. 1C top). When histology was examined by H&E staining, cellular vacuolization was observed in the AKI mice (Fig. 1C, middle), which turned out to be lipid accumulation as confirmed by the Oil-red O staining (Fig. 1C, bottom). Biochemical analysis of the lipids showed that the liver triglyceride and cholesterol levels were increased by two-fold in the AKI group, but the circulating levels of triglycerides and cholesterol were not significantly affected (Fig. 1D). In addition, the AKI mice developed acute hepatic dysfunction as evidenced by elevated plasma levels of ALT, AST and total bilirubin (Fig. 1E).

### *Renal IR decreases the hepatic expression of CAR*

To understand the molecular mechanism by which renal IR induces hepatic steatosis, microarray was performed using a pooled liver sample from three mice in each group. The microarray data showed that the expression of nuclear receptor CAR was markedly decreased in the AKI group (data not shown), and this result was confirmed by qRT-PCR (Fig. 2A), Western blotting (Fig. 2B), and immunohistochemistry (Fig. 2C). In addition to its xenobiotic functions, CAR is also known for its role in the inhibition of hepatic steatosis (Dong et al.,

Molecular Pharmacology Fast Forward. Published on January 19, 2018 as DOI: 10.1124/mol.117.111146
This article has not been copyedited and formatted. The final version may differ from this version.



2009; Gao et al., 2009). These data led to our hypothesis that the down-regulation of CAR may have played a role in the renal IR-induced fatty liver.

***Treatment with the CAR activator TCPOBOP ameliorates renal IR-induced fatty liver***

To determine whether CAR plays a role in renal IR-induced hepatic steatosis, mice were treated with the CAR activator TCPOBOP (1 mg/kg) for two days before challenging them with the renal IR surgery. While renal IR reduced the protein level of CAR in the liver, TCPOBOP treatment substantially restored the protein expression of CAR (Fig. 3A) and induced its nuclear translocation (Fig. 3B). Interestingly, the mRNA expression of CAR remained suppressed by renal IR upon the TCPOBOP treatment, regardless TCPOBOP was administered before or after the IR surgery (Supplementary Fig. 1). The mechanism for the discrepancy between the protein and mRNA expression remains to be understood. As expected, the hepatic mRNA expression of *Cyp2b10*, a CAR target gene that was suppressed by AKI, was induced / restored by TCPOBOP (Fig. 3C). The renal IR-induced steatosis was attenuated by TCPOBOP, as evidenced by the gross appearance (Fig. 3D), H&E staining (Fig. 3E), Oil-red O staining (Fig. 3F), and biochemical analysis of the hepatic and serum lipids (Fig. 3G). Of note, compared with the vehicle-treated sham mice, TCPOBOP-treated sham mice had a modest but significantly higher level of lipids (Fig. 3G), which might be secondary to the hepatomegaly effect of TCPOBOP or due to a decreased fatty acid oxidation because the expression of *PPARα* and *Cpt1α* was reduced in TCPOBOP-treated group (Supplementary Fig. 2), which was consistent with our previous report (Gao et al., 2009). In addition to relieving steatosis, treatment with TCPOBOP also improved liver function as evidenced by the normalized levels of AST, ALT and total bilirubin (Fig. 3H).

***Activation of CAR blocks the inhibitory effects of renal IR on VLDL-TG secretion***

To understand the molecular mechanisms underlying the renal IR-induced fatty liver, we investigated the effects of renal IR on hepatic gene expression with emphasis on genes associated with lipid metabolism. We found that the mRNA expression of the microsomal triglyceride transfer protein (Mttp) was significantly decreased in the AKI mice (data not shown), which was verified at the protein level by Western blotting (Fig. 4A). MTTP is necessary for the transfer of triglyceride and cholesteryl ester and the VLDL-TG secretion (Wetterau et al., 1997). It has been shown that down-regulation of MTTP increases the susceptibility to hepatic steatosis due to decreased VLDL-TG secretion (Minehira et al., 2008). The serum level of apoB100, the main structural component of VLDL (Davidson and Shelness, 2000), was also decreased in the AKI mice (Fig. 4B). We then measured the VLDL-TG secretion in mice that had been injected with tyloxapol, a lipase inhibitor. The results showed that VLDL-TG secretion was substantially reduced in vehicle-treated AKI mice compared with vehicle-treated sham mice, but the inhibitory effect of AKI on VLDL-TG secretion was abolished by the treatment of TCPOBOP (Fig. 4C). Interestingly, in the sham groups, treatment with TCPOBOP resulted in a decrease in the basal VLDL-TG secretion compared to vehicle-treated sham mice, which indicated an inhibitory effect of CAR on VLDL-TG secretion (Fig. 4C). Consistent with the results of VLDL-TG secretion, treatment with TCPOBOP abolished the AKI-responsive suppression of hepatic protein expression of Mttp (Fig. 4A) and the serum level of apoB100 (Fig. 4B).

***The attenuation of renal IR-induced fatty liver by TCPOBOP is abolished in CAR$^{-/-}$ mice***

To assess whether the hepato-protective effect of TCPOBOP is CAR dependent, CAR$^{-/-}$ mice were treated with TCPOBOP for two days before receiving the renal IR surgery. Renal IR was effective in inducing fatty liver and liver injury in the CAR$^{-/-}$ mice as shown by the liver gross appearance (Fig. 5A), H&E staining (Fig. 5B), Oil-red O staining (Fig. 5C), and liver

and serum lipid analysis (Fig. 5D). The renal IR-induced fatty liver in $CAR^{-/-}$ mice was not improved by the TCPOBOP treatment (Fig. 5A-5D). Treatment of $CAR^{-/-}$ mice with TCPBOP had little effect in relieving the liver injury either, as evidenced by the measurements of AST, ALT, and total bilirubin levels (Fig. 5E). Renal IR also suppressed VLDL-TG secretion (Fig. 5F) and decreased the serum level of apoB100 (Fig. 5G) in the $CAR^{-/-}$ mice, and these effects were not affected by the treatment of TCPOBOP.

***Activation of CAR attenuates renal IR-induced kidney injury***

It has been reported that steatosis and the severity of steatosis in kidney transplant recipients were positively correlated with the serum creatinine levels (Glicklich et al., 1999; Mikolasevic et al., 2014), suggesting that steatosis has a negative effect on the function of transplanted kidneys. Knowing IR is an integral part of a kidney transplant and activation of CAR can attenuate renal IR responsive hepatic steatosis, we went on to test whether activation of CAR can protect the kidney from IR-induced injury. In this experiment, WT mice were treated with TCPOBOP for two days before receiving the renal IR surgery, and the mice were sacrificed and analyzed 48 h later. Again, in this regimen, TCPOBOP treatment attenuated the renal IR responsive hepatic lipid accumulation, as confirmed by H&E staining (Fig. 6A), Oil-red O staining (Fig. 6B), and liver and serum lipid analysis (Fig. 6C). To our surprise, TCPOBOP-treated AKI mice also showed improvement of kidney function as indicated by their lower levels of serum creatinine and BUN compared to their vehicle-treated counterparts (Fig. 6D). At the histological level, TCPOBOP treatment reduced renal tubular damage and necrosis as shown by H&E (Fig. 6E). Tubular epithelial cell apoptosis was measured and quantified by TUNEL staining. As shown in Fig. 6F, apoptotic nuclei were abundant in vehicle-treated AKI mice, whereas the TCPOBOP treatment significantly reduced the number of TUNEL-positive cells (Fig. 6F). Western blot analysis showed that

Molecular Pharmacology Fast Forward. Published on January 19, 2018 as DOI: 10.1124/mol.117.111146
This article has not been copyedited and formatted. The final version may differ from this version.



renal IR responsive expression of neutrophil gelatinase-associated lipocalin (Ngal), a biomarker of acute kidney injury (Shemin and Dworkin, 2011), was decreased in TCPOBOP-treated mice (Fig. 6G), as was the cleavage of caspase 3 (Fig. 6G). Compared to the liver, the expression of CAR was negligible in the kidney as shown by qRT-PCR and Western blotting (Supplementary Fig. 3), consistent with a previous report (Choi et al., 1997).

***CAR ablation sensitizes mice to renal IR-induced lethality***

To determine whether CAR ablation affected an animal's sensitivity to renal IR-induced lethality, WT and $CAR^{-/-}$ mice were subjected to the 30-min ischemia / 48-h reperfusion model. While all WT mice survived the renal IR, nearly 50% of the $CAR^{-/-}$ mice died after 48 h (Fig. 7A). Histological analysis (Fig. 7B) and TUNEL (Fig. 7C) staining showed greater tubular injury in the surviving $CAR^{-/-}$ mice compared to their WT counterparts.

***Renal IR responsive increase of serum IL-6 is a potential mechanism for the renal IR-induced fatty liver and liver injury***

Inflammatory cytokines and chemokines have been proposed to be the potential mediators of distant organ injury after AKI. It has been suggested that IL-6 may have contributed to lung and liver injury after renal ischemia or bilateral nephrectomy in mice (Klein et al., 2008; Park et al., 2011). We then hypothesized that elevation of tissue and serum levels of IL-6 may have mediated the renal IR-induced fatty liver and liver injury. Indeed, renal IR increased the mRNA expression of IL-6 in both the kidney and liver (Fig. 8A), as well as the serum level of IL-6 (Fig. 8B) in the 30-min ischemia / 48-h reperfusion model. Consistent with the renal and hepato-protective effect of TCPOBOP, the TCPOBOP-treated AKI mice showed decreased renal and hepatic mRNA expression of IL-6 (Fig. 8A) and serum level of IL-6 (Fig. 8B). In the 30-min ischemia / 24-h reperfusion model, the serum level of IL-6 in the $CAR^{-/-}$ mice was

also increased but the level was comparable to that in the WT mice (Fig. 8C), likely because the IL-6 response was maximized. We also showed that treatment of primary hepatocytes with IL-6 suppressed the expression of CAR (Fig. 8D), consistent with a previous report (Pascussi et al., 2000), and this inhibitory effect of IL-6 on the expression of CAR was abolished upon the TCPOBOP treatment (Fig. 8D). Treatment with IL-6 also inhibited the constitutive and TCPOBOP responsive activity of CAR in a transient transfection and luciferase reporter gene assay (Fig. 8E). As summarized in Fig. 8F, our data suggest that IL-6 may have mediated the renal IR-induced fatty liver and liver injury through the down-regulation of the expression and activity of CAR.

Molecular Pharmacology Fast Forward. Published on January 19, 2018 as DOI: 10.1124/mol.117.111146
This article has not been copyedited and formatted. The final version may differ from this version.



## Discussion

Our results showed that renal IR-induced AKI has a distant effect in causing hepatic steatosis and liver injury. The hepatic lipid accumulation may have resulted from decreased expression and activity of CAR and inhibition of VLDL-TG secretion. Pharmacological activation of CAR by TCPOBOP prevented the development of renal IR-induced fatty liver. In contrast, $CAR^{-/-}$ mice showed fatty liver after renal IR, which could not be relieved by TCPOBOP. Alleviation of fatty liver by TCPOBOP also improved kidney function in AKI, suggesting that fatty liver can be considered as a risk factor for kidney injury. We also identified IL-6 as an important mediator for AKI-responsive inhibition of CAR and development of fatty liver.

To our knowledge, this is the first demonstration that renal IR induces CAR down-regulation and steatosis in the liver. Although several studies have reported hepatic cellular vacuolization upon renal IR (Golab et al., 2009; Pelletier et al., 2013; Rabadi et al., 2016), understanding the mechanism of renal IR-induced fatty liver has been limited. Most published studies emphasize inflammatory responses, apoptosis, and necrosis in the liver after renal injury. For example, renal peptidyl arginine deiminase-4 (PAD4) increases the renal tubular inflammatory response after renal IR by interacting with NF-κB (Rabadi et al., 2016). Genetic ablation of PAD4 attenuates AKI-induced kidney injury and liver injury. In this study, we showed that hepatic steatosis is an acute response to renal IR. Renal IR-induced CAR down-regulation in the liver resulted in a decreased expression of Mttp, leading to reduced VLDL-TG secretion. Treatment with TCPOBOP abolished the inhibitory effect of renal IR on VLDL-TG secretion and thus decreased lipid accumulation. The mechanism by which CAR blocks the inhibitory effect of renal IR on VLDL-TG secretion remains to be fully understood. Nevertheless, the attenuation of renal IR-induced fatty liver by TCPOBOP is consistent with the anti-steatotic activity of CAR (Dong et al., 2009; Gao et al., 2009).

Our findings that renal IR-induced fatty liver and attenuation of fatty liver helped preserving kidney function have their clinical implications. Renal transplant recipients have been reported to have a higher prevalence of fatty liver compared to the general population (Mikolasevic et al., 2014). Moreover, fatty liver in renal transplant patients was found to have a negative impact on the function of the grafted kidneys. The severity of fatty liver correlated with elevated serum creatinine levels and decreased estimated glomerular filtration rate in renal transplant patients (Anuras et al., 1977; Mikolasevic et al., 2014). In this study, $CAR^{-/-}$ mice were found to be more sensitive to renal IR injury and renal IR induced lethality, which was likely due to a higher basal triglyceride content in the liver. The spontaneous steatosis in the $CAR^{-/-}$ mice may have resulted from the de-suppression of the lipogenic nuclear receptor liver X receptor (Zhai et al., 2010). In contrast, pharmacological activation of CAR alleviated fatty liver and improved the renal function in AKI. Our results support the notion that fatty liver might be an important risk factor contributing to the development of renal graft dysfunction. Meanwhile, CAR can be explored as a therapeutic target to manage fatty liver and to avoid graft dysfunction in renal transplant patients. Since the expression of CAR in the kidney was negligible, we reason the nephro-protective effect of TCPOBOP was likely due to the hepatic activation of CAR.

Mechanistically, our results suggested the renal IR-induced inflammatory cytokines may have mediated the distal effect of AKI on the liver. Among the inflammatory cytokines, IL-6 plays an important role in AKI-induced distant organ injury (Klein et al., 2008; Park et al., 2011). Elevated levels of serum IL-6 were observed after ischemic AKI and bilateral nephrectomy (Klein et al., 2008). Increases in serum IL-6 have been reported in hospitalized AKI patients and the level of serum IL-6 showed a significant association with increased mortality

(Simmons et al., 2004). IL-6 is known to inhibit the expression of CYP2 and CYP3 genes (Abdel-Razzak et al., 1993; Morgan et al., 2008; Muntane-Relat et al., 1995; Pascussi et al., 2000), likely by decreasing the expression and/or activity of CAR. The elevated hepatic and systemic level of IL-6 may have accounted for the suppression of CAR in the AKI liver. In contrast, treatment with TCPOBOP decreased the hepatic, renal and circulating levels of IL-6, which helped the recovery of the expression and activity of CAR in the liver, leading to the relief of hepatic and renal injury. The inhibitory effect of TCPOBOP on IL-6 was consistent with the notion that activation of CAR can attenuate inflammation in several disease models (Cheng et al., 2017; Shah et al., 2014).

Another potential implication of our study is that AKI can change hepatic drug metabolism through the down-regulation of CAR, a master regulator of drug metabolism. Because the pharmacokinetics and pharmacodynamics of drugs are altered in critically ill patients, dose adjustment is often necessary. CYP-mediated drug metabolism is a critical issue in patients of AKI due to an altered efficacy or toxicity of drugs. However, the impact of AKI on hepatic drug metabolism is not well documented. Midazolam exhibits a prolonged action in AKI patients due to decreased CYP3A4/5-mediated hepatic metabolism as well as diminished renal excretion (Kirwan et al., 2012). Antipyrine and losartan showed a decrease in metabolism by CYP2B6 and CYP2C9 in animal models of renal IR, bilateral ureteric ligation, and uranyl nitrate injury (Gurley et al., 1997; Yoshitani et al., 2002). The expression of CYP3A4/5, CYP2B6, and CYP2C9 is under the transcriptional control by CAR and its sister xenobiotic receptor pregnane X receptor (PXR) (Gerbal-Chaloin et al., 2002; Xie et al., 2000). Because CAR can also regulate the expression of phase II conjugating enzymes and drug transporters, all stages of hepatic drug metabolism can potentially be affected by AKI due to the suppression of CAR (Maglich et al., 2002; Xie et al., 2000).

Molecular Pharmacology Fast Forward. Published on January 19, 2018 as DOI: 10.1124/mol.117.111146
This article has not been copyedited and formatted. The final version may differ from this version.



In summary, we have uncovered a novel function of CAR in mediating the crosstalk between the injured kidney and liver. Activation of CAR relieved renal IR-induced fatty liver and kidney injury, whereas CAR ablation sensitized mice to renal IR-induced AKI. Knowing that kidney transplant recipients have a higher incidence of fatty liver and fatty liver has a negative effect on the function of grafted kidneys, it is tempting to speculate that CAR can be explored as a therapeutic target to manage fatty liver and to avoid graft dysfunction in renal transplant patients.

## Authorship contributions

Participated in research design: Choi and Xie.

Conducted experiments: Choi, Zhou, Barbosa, Niu, Guan, Xu, and Ren.

Performed data analysis: Choi and Xie.

Wrote or contributed to writing of the manuscript: Choi, Guan, Nolin., Liu, and Xie.

## References

Abdel-Razzak Z, Loyer P, Fautrel A, Gautier JC, Corcos L, Turlin B, Beaune P and Guillouzo A (1993) Cytokines down-regulate expression of major cytochrome P-450 enzymes in adult human hepatocytes in primary culture. *Mol Pharmacol* **44**: 707-715.

Anuras S, Piros J, Bonney WW, Forker EL, Colville DS and Corry RJ (1977) Liver disease in renal transplant recipients. *Arch Intern Med* **137**: 42-48.

Assenat E, Gerbal-Chaloin S, Larrey D, Saric J, Fabre JM, Maurel P, Vilarem MJ and Pascussi JM (2004) Interleukin 1beta inhibits CAR-induced expression of hepatic genes involved in drug and bilirubin clearance. *Hepatology* **40**: 951-960.

Axelsson J, Astrom G, Sjolin E, Qureshi AR, Lorente-Cebrian S, Stenvinkel P and Ryden M (2011) Uraemic sera stimulate lipolysis in human adipocytes: role of perilipin. *Nephrol Dial Transplant* **26**: 2485-2491.

Cheng S, Zou M, Liu Q, Kuang J, Shen J, Pu S, Chen L, Li H, Wu T, Li R, Li Y, Jiang W, Zhang Z and He J (2017) Activation of Constitutive Androstane Receptor Prevents Cholesterol Gallstone Formation. *Am J Pathol* **187**: 808-818.

Chertow GM, Christiansen CL, Cleary PD, Munro C and Lazarus JM (1995) Prognostic stratification in critically ill patients with acute renal failure requiring dialysis. *Arch Intern Med* **155**: 1505-1511.

Choi HS, Chung M, Tzameli I, Simha D, Lee YK, Seol W and Moore DD (1997) Differential transactivation by two isoforms of the orphan nuclear hormone receptor CAR. *J Biol Chem* **272**: 23565-23571.

Davidson NO and Shelness GS (2000) APOLIPOPROTEIN B: mRNA editing, lipoprotein assembly, and presecretory degradation. *Annu Rev Nutr* **20**: 169-193.

Devarajan P (2006) Update on mechanisms of ischemic acute kidney injury. *J Am Soc Nephrol* **17**: 1503-1520.

Doi K and Rabb H (2016) Impact of acute kidney injury on distant organ function: recent findings and potential therapeutic targets. *Kidney Int* **89**: 555-564.

Dong B, Saha PK, Huang W, Chen W, Abu-Elheiga LA, Wakil SJ, Stevens RD, Ilkayeva O, Newgard CB, Chan L and Moore DD (2009) Activation of nuclear receptor CAR ameliorates diabetes and fatty liver disease. *Proc Natl Acad Sci U S A* **106**: 18831-18836.

Gao J, He J, Zhai Y, Wada T and Xie W (2009) The constitutive androstane receptor is an anti-obesity nuclear receptor that improves insulin sensitivity. *J Biol Chem* **284**: 25984-25992.

Gao J and Xie W (2012) Targeting xenobiotic receptors PXR and CAR for metabolic diseases. *Trends Pharmacol Sci* **33**: 552-558.

Gerbal-Chaloin S, Daujat M, Pascussi JM, Pichard-Garcia L, Vilarem MJ and Maurel P (2002) Transcriptional regulation of CYP2C9 gene. Role of glucocorticoid receptor and constitutive androstane receptor. *J Biol Chem* **277**: 209-217.

Glicklich D, Thung SN, Kapoian T, Tellis V and Reinus JF (1999) Comparison of clinical features and liver histology in hepatitis C-positive dialysis patients and renal transplant recipients. *Am J Gastroenterol* **94**: 159-163.

Golab F, Kadkhodaee M, Zahmatkesh M, Hedayati M, Arab H, Schuster R, Zahedi K, Lentsch AB and Soleimani M (2009) Ischemic and non-ischemic acute kidney injury cause hepatic damage. *Kidney Int* **75**: 783-792.

Gurley BJ, Barone GW, Yamashita K, Polston S, Estes M and Harden A (1997) Extrahepatic ischemia-reperfusion injury reduces hepatic oxidative drug metabolism as determined by serial antipyrine clearance. *Pharm Res* **14**: 67-72.

Honkakoski P, Zelko I, Sueyoshi T and Negishi M (1998) The nuclear orphan receptor CAR-retinoid X receptor heterodimer activates the phenobarbital-responsive enhancer

module of the CYP2B gene. *Mol Cell Biol* **18**: 5652-5658.

Khwaja A (2012) KDIGO clinical practice guidelines for acute kidney injury. *Nephron Clin Pract* **120**: c179-184.

Kirwan CJ, MacPhee IA, Lee T, Holt DW and Philips BJ (2012) Acute kidney injury reduces the hepatic metabolism of midazolam in critically ill patients. *Intensive Care Med* **38**: 76-84.

Klein CL, Hoke TS, Fang WF, Altmann CJ, Douglas IS and Faubel S (2008) Interleukin-6 mediates lung injury following ischemic acute kidney injury or bilateral nephrectomy. *Kidney Int* **74**: 901-909.

Maglich JM, Stoltz CM, Goodwin B, Hawkins-Brown D, Moore JT and Kliewer SA (2002) Nuclear pregnane x receptor and constitutive androstane receptor regulate overlapping but distinct sets of genes involved in xenobiotic detoxification. *Mol Pharmacol* **62**: 638-646.

Mikolasevic I, Racki S, Lukenda V, Milic S, Pavletic-Persic M and Orlic L (2014) Nonalcoholic Fatty liver disease in renal transplant recipients proven by transient elastography. *Transplant Proc* **46**: 1347-1352.

Minehira K, Young SG, Villanueva CJ, Yetukuri L, Oresic M, Hellerstein MK, Farese RV, Jr., Horton JD, Preitner F, Thorens B and Tappy L (2008) Blocking VLDL secretion causes hepatic steatosis but does not affect peripheral lipid stores or insulin sensitivity in mice. *J Lipid Res* **49**: 2038-2044.

Morgan ET, Goralski KB, Piquette-Miller M, Renton KW, Robertson GR, Chaluvadi MR, Charles KA, Clarke SJ, Kacevska M, Liddle C, Richardson TA, Sharma R and Sinal CJ (2008) Regulation of drug-metabolizing enzymes and transporters in infection, inflammation, and cancer. *Drug Metab Dispos* **36**: 205-216.

Muntane-Relat J, Ourlin JC, Domergue J and Maurel P (1995) Differential effects of

cytokines on the inducible expression of CYP1A1, CYP1A2, and CYP3A4 in human hepatocytes in primary culture. *Hepatology* **22**: 1143-1153.

Musso G, Gambino R, Tabibian JH, Ekstedt M, Kechagias S, Hamaguchi M, Hultcrantz R, Hagstrom H, Yoon SK, Charatcharoenwitthaya P, George J, Barrera F, Hafliethadottir S, Bjornsson ES, Armstrong MJ, Hopkins LJ, Gao X, Francque S, Verrijken A, Yilmaz Y, Lindor KD, Charlton M, Haring R, Lerch MM, Rettig R, Volzke H, Ryu S, Li G, Wong LL, Machado M, Cortez-Pinto H, Yasui K and Cassader M (2014) Association of non-alcoholic fatty liver disease with chronic kidney disease: a systematic review and meta-analysis. *PLoS Med* **11**: e1001680.

Park SW, Chen SW, Kim M, Brown KM, Kolls JK, D'Agati VD and Lee HT (2011) Cytokines induce small intestine and liver injury after renal ischemia or nephrectomy. *Lab Invest* **91**: 63-84.

Park SW, Kim M, Kim JY, Ham A, Brown KM, Mori-Akiyama Y, Ouellette AJ, D'Agati VD and Lee HT (2012) Paneth cell-mediated multiorgan dysfunction after acute kidney injury. *J Immunol* **189**: 5421-5433.

Pascussi JM, Gerbal-Chaloin S, Pichard-Garcia L, Daujat M, Fabre JM, Maurel P and Vilarem MJ (2000) Interleukin-6 negatively regulates the expression of pregnane X receptor and constitutively activated receptor in primary human hepatocytes. *Biochem Biophys Res Commun* **274**: 707-713.

Pelletier CC, Koppe L, Croze ML, Kalbacher E, Vella RE, Guebre-Egziabher F, Geloen A, Badet L, Fouque D and Soulage CO (2013) White adipose tissue overproduces the lipid-mobilizing factor zinc alpha2-glycoprotein in chronic kidney disease. *Kidney Int* **83**: 878-886.

Rabadi M, Kim M, D'Agati V and Lee HT (2016) Peptidyl arginine deiminase-4-deficient mice are protected against kidney and liver injury after renal ischemia and reperfusion.

*Am J Physiol Renal Physiol* **311**: F437-449.

Rewa O and Bagshaw SM (2014) Acute kidney injury-epidemiology, outcomes and economics. *Nat Rev Nephrol* **10**: 193-207.

Shah P, Guo T, Moore DD and Ghose R (2014) Role of constitutive androstane receptor in Toll-like receptor-mediated regulation of gene expression of hepatic drug-metabolizing enzymes and transporters. *Drug Metab Dispos* **42**: 172-181.

Shang Y, Siow YL, Isaak CK and O K (2016) Downregulation of Glutathione Biosynthesis Contributes to Oxidative Stress and Liver Dysfunction in Acute Kidney Injury. *Oxid Med Cell Longev* **2016**: 9707292.

Shemin D and Dworkin LD (2011) Neutrophil gelatinase-associated lipocalin (NGAL) as a biomarker for early acute kidney injury. *Crit Care Clin* **27**: 379-389.

Shi Y, Melnikov VY, Schrier RW and Edelstein CL (2000) Downregulation of the calpain inhibitor protein calpastatin by caspases during renal ischemia-reperfusion. *Am J Physiol Renal Physiol* **279**: F509-517.

Simmons EM, Himmelfarb J, Sezer MT, Chertow GM, Mehta RL, Paganini EP, Soroko S, Freedman S, Becker K, Spratt D, Shyr Y and Ikizler TA (2004) Plasma cytokine levels predict mortality in patients with acute renal failure. *Kidney Int* **65**: 1357-1365.

Targher G and Byrne CD (2017) Non-alcoholic fatty liver disease: an emerging driving force in chronic kidney disease. *Nat Rev Nephrol* **13**: 297-310.

Venkatachalam MA, Weinberg JM, Kriz W and Bidani AK (2015) Failed Tubule Recovery, AKI-CKD Transition, and Kidney Disease Progression. *J Am Soc Nephrol* **26**: 1765-1776.

Wei P, Zhang J, Egan-Hafley M, Liang S and Moore DD (2000) The nuclear receptor CAR mediates specific xenobiotic induction of drug metabolism. *Nature* **407**: 920-923.

Wetterau JR, Lin MC and Jamil H (1997) Microsomal triglyceride transfer protein. *Biochim*

*Biophys Acta* **1345**: 136-150.

Wu H, Chen G, Wyburn KR, Yin J, Bertolino P, Eris JM, Alexander SI, Sharland AF and Chadban SJ (2007) TLR4 activation mediates kidney ischemia/reperfusion injury. *J Clin Invest* **117**: 2847-2859.

Xie W, Barwick JL, Simon CM, Pierce AM, Safe S, Blumberg B, Guzelian PS and Evans RM (2000) Reciprocal activation of xenobiotic response genes by nuclear receptors SXR/PXR and CAR. *Genes Dev* **14**: 3014-3023.

Yoshitani T, Yagi H, Inotsume N and Yasuhara M (2002) Effect of experimental renal failure on the pharmacokinetics of losartan in rats. *Biol Pharm Bull* **25**: 1077-1083.

Zhai Y, Wada T, Zhang B, Khadem S, Ren S, Kuruba R, Li S and Xie W (2010) A functional cross-talk between liver X receptor-alpha and constitutive androstane receptor links lipogenesis and xenobiotic responses. *Mol Pharmacol* **78**: 666-674.

**Footnotes**

The work was supported in part by the National Institutes of Health [Grants DK083952, ES023438].

## Figure Legends

**Fig. 1.** ***Renal IR induces hepatic steatosis***

**(A)** C57BL/6 male mice were subjected to sham surgery or 30 min of bilateral renal ischemia followed by 24 h of reperfusion. Blood samples were collected to measure serum levels of creatinine and BUN. **(B)** Renal histology as shown by H&E staining. The original magnification is 200×. Arrow and arrowhead indicate tubular dilation and necrosis, respectively. **(C)** Macroscopic liver appearance (top) and liver histology as shown by H&E staining (middle) and Oil-Red O staining (bottom). **(D)** The hepatic and serum lipid levels. **(E)** Serum ALT, AST and total bilirubin levels. Results are presented as mean ± SD of five mice per group. *, $p<0.05$, compared to the sham group.

**Fig. 2.** ***Renal IR decreases the hepatic expression of CAR***

Mice were the same as described in Fig. 1. **(A)** Liver *CAR* mRNA expression was measured by qRT-PCR. The relative gene levels are represented as fold change compared to the sham group. Results are presented as mean ± SD of five mice per group. *, $p<0.05$, compared to the sham group. **(B)** Liver CAR protein expression was measured by Western blotting. Lanes represent individual mice. Shown on the top right is the densitometric quantification of the Western blotting results. **(C)** Liver CAR protein expression was detected by immunohistochemistry. Arrowheads indicate positive staining.

**Fig. 3.** ***Treatment with the CAR activator TCPOBOP ameliorates renal IR-induced fatty liver***

C57BL/6 male mice were randomly assigned into four groups. Two treatment groups were administered with TCPOBOP for two days (1 mg/kg BW/day; i.p.) before receiving the sham surgery or renal IR 24 h after the last doses of drugs. Two vehicle groups received the same

volume of corn oil for two days before receiving the sham surgery or renal IR. **(A)** Liver CAR protein expression was measured by Western blotting. Shown on the bottom left is the densitometric quantification of the Western blotting results. **(B)** Liver CAR protein expression was detected by immunohistochemistry. Arrowheads indicate positive staining. **(C)** *Cyp2b10* mRNA expression was measured by qRT-PCR. The relative gene levels are represented as fold change compared to vehicle-treated sham group. **(D-F)** Macroscopic liver appearance (D) and liver histology as shown by H&E (E) and Oil-Red O staining (F). **(G)** The hepatic and serum lipid levels. **(H)** Serum ALT, AST and total bilirubin levels. Results are presented as mean ± SD of five mice per group. *, $p<0.05$, with the comparisons labeled.

**Fig. 4.** ***Activation of CAR blocks the inhibitory effects of renal IR on VLDL-TG secretion***

Mice were the same as described in Fig. 3. **(A)** Liver Mttp protein expression was measured by Western blotting. Shown on the right is the densitometric quantification of the Western blotting results. Each bar represents the mean ± SD of five mice. **(B)** Serum Apob100 level was detected by Western blotting. Ponceau S staining was used as a loading control. **(C)** VLDL-TG secretion assay. Mice were fasted for 4 h before receiving an intravenous injection of tyloxapol (500 mg/kg body weight). Blood samples were collected at 0, 30, 60, and 120 min and measured for serum concentrations of triglycerides. Each bar represents the mean ± SD of three mice. *, $p<0.05$, with the comparisons labeled.

**Fig. 5.** ***The attenuation of renal IR-induced fatty liver by TCPOBOP is abolished in CAR$^{-/-}$ mice***

The experimental designs were the same described in Fig. 3 except that male CAR$^{-/-}$ mice were used. **(A-C)** Macroscopic liver appearance (A) and liver histology as shown by H&E (B) and Oil-Red O staining (C). **(D)** The hepatic and serum lipid levels. **(E)** Serum ALT, AST and

total bilirubin levels. **(F)** VLDL-TG secretion assay. **(G)** Serum Apob100 was detected by Western blotting. Ponceau S staining was used as a loading control. Each bar represents the mean ± SD of five mice. *, $p<0.05$, with the comparisons labeled.

**Fig. 6.** ***Activation of CAR attenuates renal IR-induced kidney injury***

WT C57BL/6 male mice were randomly assigned, and treatment groups were administered with TCPOBOP for two days (1 mg/kg BW/day; i.p.). Vehicle groups received the same volume of corn oil. Mice received the renal IR surgery or sham surgery 24h after the last dose of drugs and sacrificed 48h after the renal IR. **(A and B)** liver histology as shown by H&E (A) and Oil-Red O staining (B). **(C)** The hepatic and serum lipid levels. **(D)** The serum creatinine and BUN levels. **(E)** Renal histology as shown by H&E staining. Arrows and arrowheads indicate tubular dilation and necrosis, respectively. **(F)** TUNEL staining to identify apoptotic renal cells (green fluorescence). DAPI staining of cell nuclei is shown in blue. Shown below is the quantification of the TUNEL-positive cells from three mice in each group. The abrupt change in contrast from left to right may have resulted from an artifact in the detector; t he image has not been spliced. **(G)** Western blot analysis to detect the protein expression of Ngal, total Caspase3, and cleaved Caspase3 in the mouse kidneys. Each bar represents the mean ± SD of five mice. *, $p<0.05$, with the comparisons labeled.

**Fig. 7.** ***CAR ablation sensitizes mice to renal IR-induced lethality***

WT and $CAR^{-/-}$ mice were renal IR or sham surgery as described in Fig. 6. **(A)** Animal survival curve. **(B)** Renal histology as shown by H&E staining. Arrows and arrowheads indicate tubular dilation and necrosis, respectively. **(C)** TUNEL staining to identify apoptotic renal cells (green fluorescence). DAPI staining of cell nuclei is shown in blue. Shown on the right is the quantification of the TUNEL-positive cells from three mice in each group. The ab

Molecular Pharmacology Fast Forward. Published on January 19, 2018 as DOI: 10.1124/mol.117.111146
This article has not been copyedited and formatted. The final version may differ from this version.



rupt change in contrast from left to right may have resulted from an artifact in the detec tor; the image has not been spliced. *, $p<0.05$, with the comparisons labeled.

**Fig. 8.** ***Renal IR responsive increase of serum IL-6 is a potential mechanism for the renal IR-induced fatty liver and liver injury***

**(A and B)** Mice were subjected to the 30-min ischemia / 48-h reperfusion model. The *IL-6* mRNA expression in the kidney and liver was determined by qRT-PCR (A) and the serum IL-6 levels were measured by ELISA (B). Each bar represents the mean ± SD of five mice. **(C)** The serum IL-6 levels were measured in WT and $CAR^{-/-}$ mice that were subjected to the 30-min ischemia / 24-h reperfusion model. **(D)** Mouse primary hepatocytes were isolated and incubated with IL-6 (50 U/mL) in the presence or absence of TCPOBOP (200 nM) for 24 h. The mRNA expression of CAR was measured by qRT-PCR. **(E)** HEK293T cells were transiently transfected with the mouse CAR expression vector pCMX-HA-mCAR and the CAR responsive tk-PBRE reporter plasmid. Transfected cells were incubated with IL-6 (50 U/mL) in the presence or absence of TCPOBOP (200 nM) for 24 h before cell harvesting and luciferase assay. *, $p<0.05$, with the comparisons labeled. **(F)** Proposed mechanisms of renal IR-induced fatty liver and liver injury. Elevation of serum IL-6 after AKI mediates renal IR-induced kidney and liver injury through CAR down-regulation.

Fig. 1

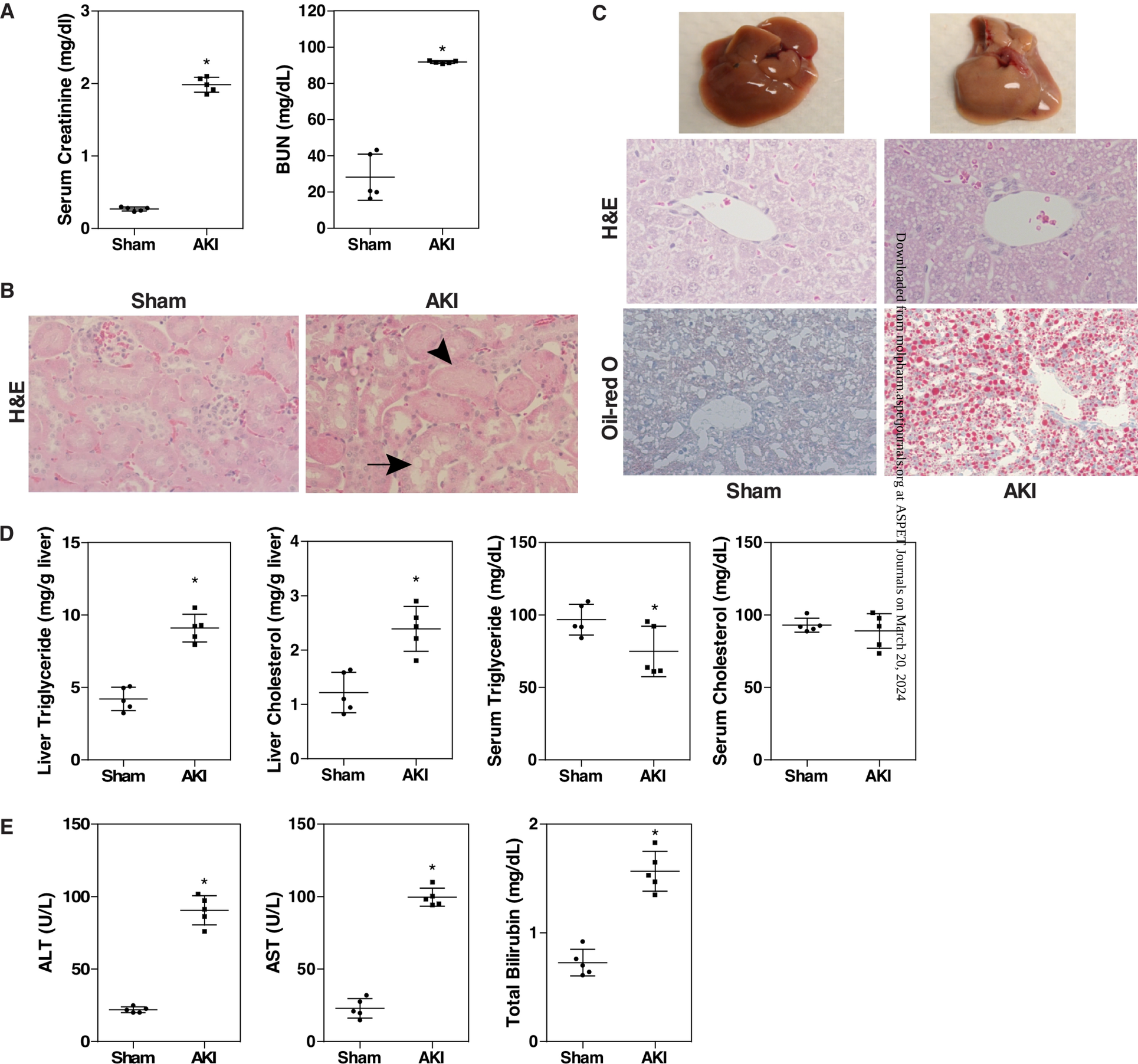

Molecular Pharmacology Fast Forward. Published on January 19, 2018 as DOI: 10.1124/mol.117.111146
This article has not been copyedited and formatted. The final version may differ from this version.

Fig. 2

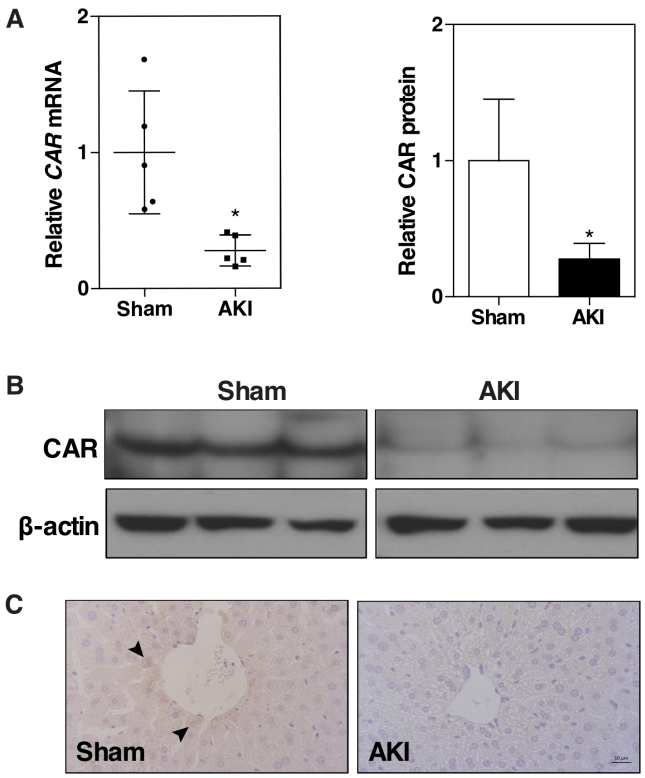

Fig. 3

Molecular Pharmacology Fast Forward. Published on January 19, 2018 as DOI: 10.1124/mol.117.111146
This article has not been copyedited and formatted. The final version may differ from this version.

Fig. 4

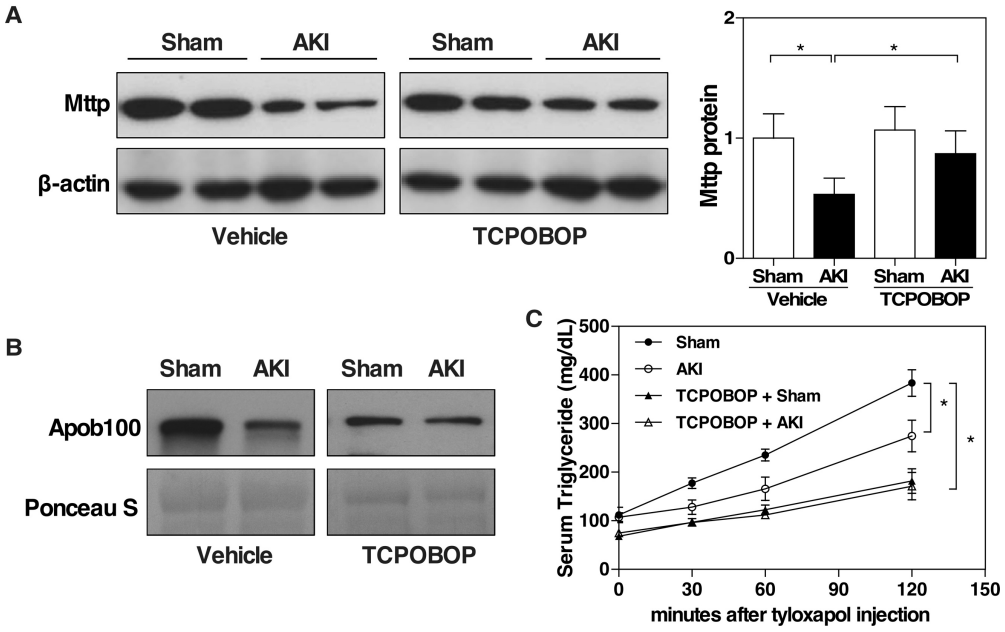

Molecular Pharmacology Fast Forward. Published on January 19, 2018 as DOI: 10.1124/mol.117.111146
This article has not been copyedited and formatted. The final version may differ from this version.

Fig. 5

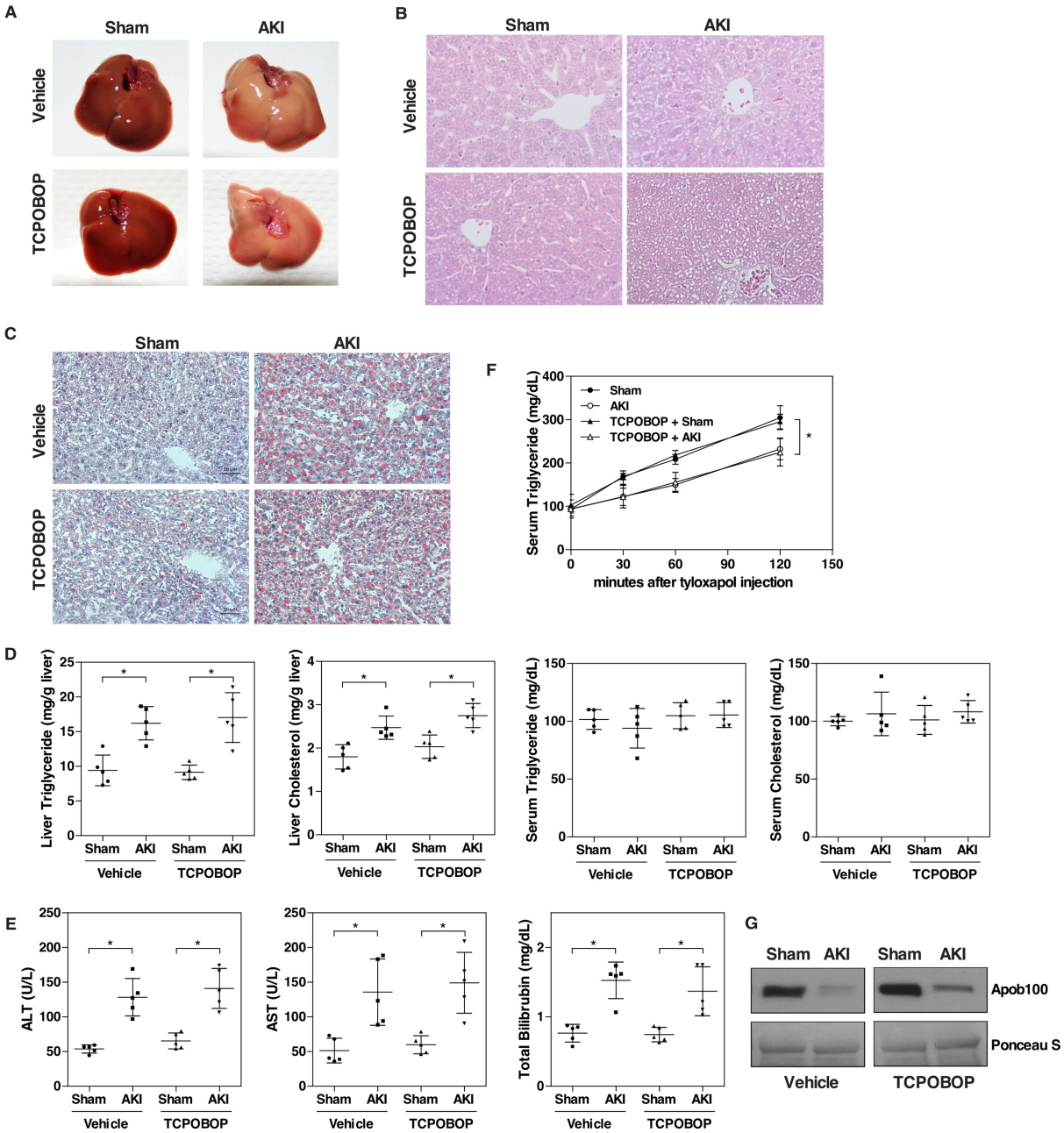

Molecular Pharmacology Fast Forward. Published on January 19, 2018 as DOI: 10.1124/mol.117.111146
This article has not been copyedited and formatted. The final version may differ from this version.

Fig. 6

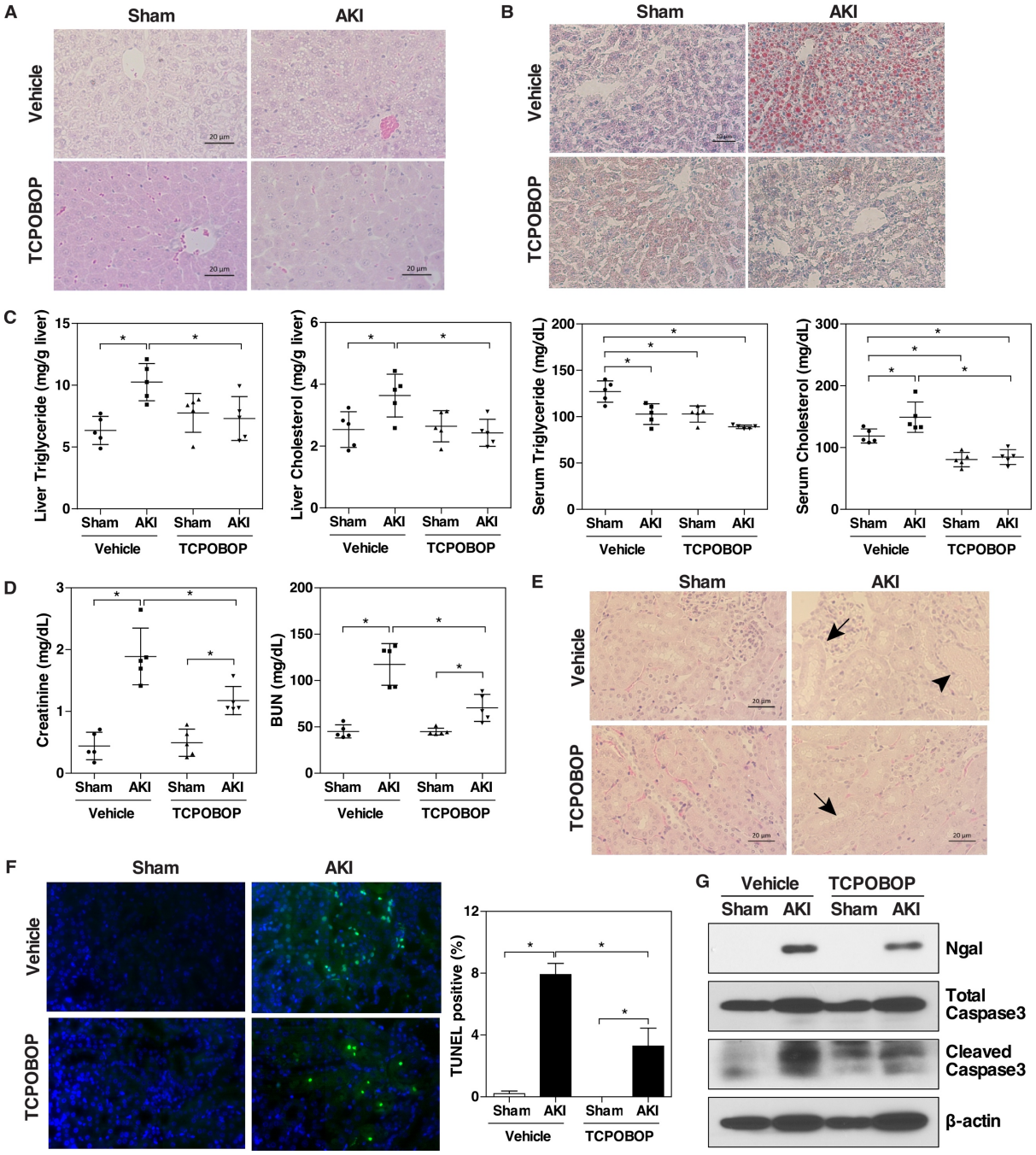

Molecular Pharmacology Fast Forward. Published on January 19, 2018 as DOI: 10.1124/mol.117.111146
This article has not been copyedited and formatted. The final version may differ from this version.

Fig. 7

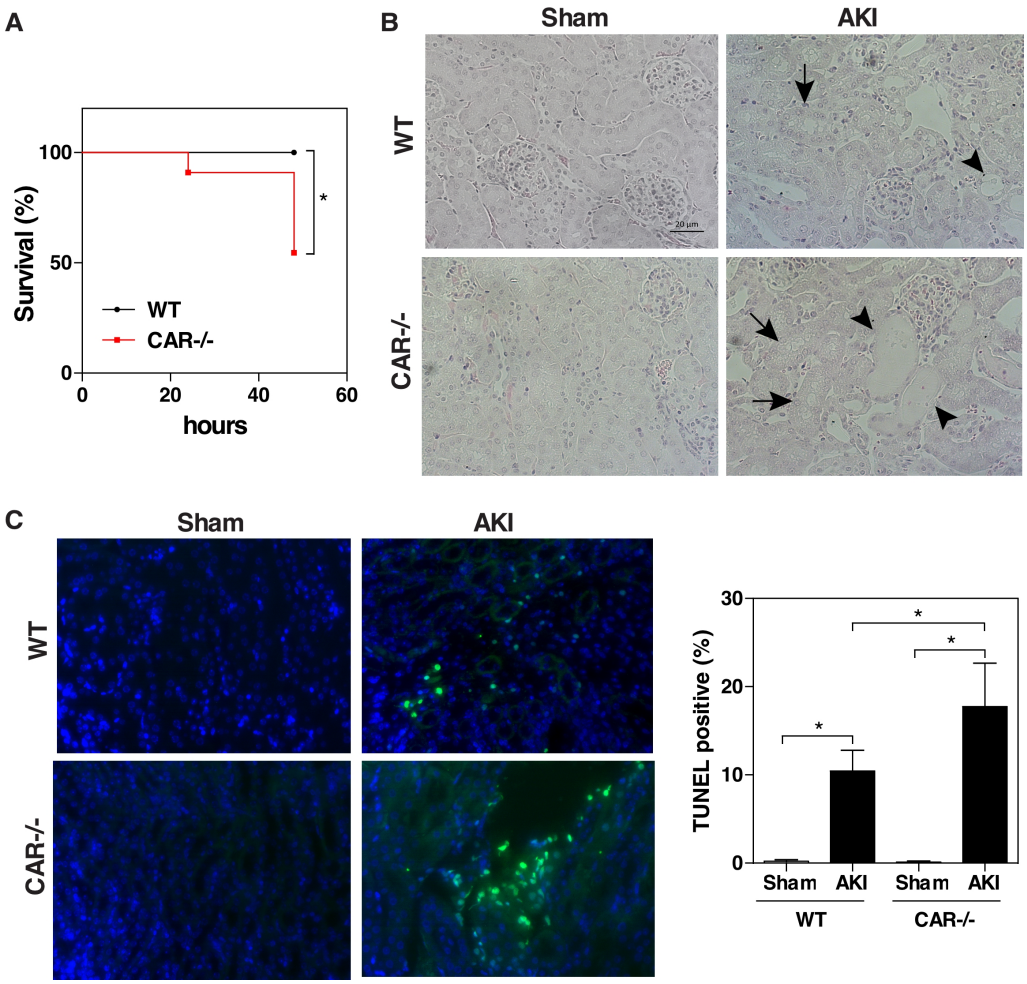

Molecular Pharmacology Fast Forward. Published on January 19, 2018 as DOI: 10.1124/mol.117.111146
This article has not been copyedited and formatted. The final version may differ from this version.

Fig. 8